Computer-Aided Design of Promising Photochemical Alkoxy Radical Precursors

Mario Arnone and Bernd Engels*

Institut für organische Chemie, Universität Wurzburg, Am Hubland, D-97074 Würzburg, Germany

Received: June 21, 2006; In Final Form: August 10, 2006

A computer-aided design of alkoxyl radical precursors is performed. The new precursors should combine the advantages of *N*-alkoxypyridine-2(*1H*)thiones (less reactive radicals) and *N*-alkoxythiazole-2(*3H*)thiones (stable with respect to daylight). Additionally, the radical liberation process should be initiated by light with a wavelength of around 350 nm. To find promising compounds, 18 test candidates were obtained by a systematic variation of the parent compound *N*-alkoxythiazole-2(*3H*)thione. The properties of the test molecules were computed by a protocol that was already successfully used to rationalize the photochemical behavior of *N*-alkoxypyridine-2(*1H*)thiones and *N*-alkoxythiazole-2(*3H*)thiones. The computations identify two promising new compounds. For *N*-methoxy-(1,3)dihydro-[1,3]azaphosphole-2-thione (**6a**), they predict that the fragmentation process will be initiated by an absorption at 348 nm. An analysis of its fragmentation process indicates that the free excess energy of the resulting radicals should more resemble the situation found for *N*-alkoxypyridine-2(*1H*)thiones. For *N*-methoxy-(1,3)dihydro-pyrrole-2-thione (**3a**), the excitation energy is somewhat higher (330 nm), but the computed fragmentation paths again indicate that the remaining excess energy of the released radicals is quite favorable. The test molecules also contained the experimentally well-known *N*-methoxypyridine-2(*1H*)one (**1b**). For this molecule, our computed data rationalizes nicely the experimental findings.

Introduction

Alkoxyl radicals are an important class of substances for photobiological,[1−4] mechanistic,[5,6] and synthetic investigations.[7,8] Well-established accesses to alkoxyl radicals use the homolytical O,O bond cleavage in perethers or organic peresters.[9−11] Drawbacks of these approaches are difficulties in the handling of these unstable systems. To avoid such difficulties newer approaches to alkoxyl radicals use UV/vis photolysis of thiohydroxamic O-esters. The irradiation with light leads to a N,O bond homolysis associated with a liberation of the oxygen-centered radicals.[12,13] *N*-alkoxypyridine-2(*1H*)thiones were the first compounds which were used in this context.[4,14] With these molecules, it was possible to generate alkoxyl radicals for a stereoselective synthesis of a muscarinalkaloid.[15] A big disadvantage of these compounds, however, is their sensibility to daylight. Due to an absorption at about 370 nm, a decomposition of the pyridinethiones occurs already when they are exposed to unfiltered daylight. Only if the blue part of the light is filtered out the *N*-alkoxypyridine-2(*1H*)thiones are stable.[16]

To eliminate this problem, substituted *N*-alkoxythiazole-2(*3H*)thiones were developed.[16] They absorb at about 330 nm so that they do not decompose when exposed to daylight. However, when irradiated with UV light without the presence of radical trapping reagents, the yield of alkoxyl radicals is very low and many unwanted side products are found.[12]

To elucidate the differences between *N*-alkoxypyridine-2(*1H*)-thiones and *N*-alkoxythiazole-2(*3H*)thione compounds in previous investigations, the electronic spectra of the precursor systems *N*-methoxypyridine-2(*1H*)thione (**1a**) and *N*-methoxythiazole-2(*3H*)thione (**2a**) were computed.[17,18] On the basis of CASPT2[19,20] computations (complete active space self-consistent field calculation together with an MP2 estimation of dynamic correlation effects), the spectroscopic visible absorption bands of both compounds were assigned to the $S_0 \rightarrow S_2$ transition. In both cases, they correspond to a $\pi \rightarrow \pi^*$ excitation in the thiocarbonyl group of the thiohydroxamic functionality.[17] The higher stabilities of the thiazolethione compounds with respect to daylight simply result because their S_2 states are higher in energy. The study also found a reason why an irradiation of *N*-alkoxythiazole-2(*3H*)thiones delivers much more reactive radicals than the irradiation of *N*-alkoxypyridine-2(*1H*)thiones. The higher reactivity in the case of the thiazole compounds may result because the potential surfaces that determine the photolytic N,O bond cleavage represent a perfect slide from the S_2 state through a conical intersection into the S_1 and then into the final ground state of the radical fragments. Due to the resulting fast dissociation process, the excess energy which results from the photolytic fragmentation is dissipated to the solvent only to small amounts.[21] For *N*-alkoxypyridine-2(*1H*)thiones, a dissipation of the excess energy is much more likely because its S_2 state possesses a barrier with respect to the dissociation. Additionally, no avoided crossing between S_2 and S_1 is found so that also the de-excitation process can be expected to be much slower. Finally, the maximal excess energy of the fragments is also lower. This results from a lower vertical excitation energy (starting point of the photolytic fragmentation) and a higher dissociation energy of the S_0 state. The latter determines the energy position of the resulting radicals in their ground states.

A comparison of the CASPT2 results with TD-DFT[22,23] (time-dependent density functional theory) calculations showed that only some functionals give the right quantitative answers. All applied TD-DFT methods agreed in the assignment of the visible bands, but the prediction of the vertical excitation energies differed considerably. Although the B3LYP functional[24,25]

* To whom correspondence should be addressed. Fax: +49 (0)931/888 5331; E-mail: bernd@chemie.uni-wuerzburg.de.

10.1021/jp063876m CCC: $33.50
Published on Web 10/18/2006

Z	heterocycle
CH=CH	pyridine (**1**)
S	thiazole (**2**)
CH_2	pyrrole (**3**)
NH	imidazole (**4**)
O	oxazole (**5**)
PH	phosphazole (**6**)

X	Y	functional group
S	N	thione (**a**)
O	N	ketone (**b**)
S	P	phosphonethione (**c**)

Figure 1. Structural formular and indexing of the systematically modified heterocycles.

worked well for the prediction of the visible band of pyridine compounds, it overestimated the energy position of the visible band of *N*-methoxythiazole-2(*3H*)thione by more than 0.3 eV. The BLYP functional[26] on the other hand predicts the energy position of the intensive band of *N*-methoxythiazole-2(*3H*)thione quite well but fails to predict the other bands of this compound and the spectra of *N*-methoxypyridine-2(*1H*)thione correctly.[18]

As photochemical alkoxyl radical precursors both *N*-alkoxypyridine-2(*1H*)thiones and *N*-alkoxythiazole-2(*3H*)thiones possess advantages but also disadvantages. Therefore, the question arised if it is possible to identify new lead structures for photochemical precursor systems that combine the advantages of both compounds. The dissociation behavior of new precursors should be similar to the behavior of pyridinethione compounds to avoid unwanted side reactions during the radical formation process. On the other hand, the excitation wavelength that initiates the fragmentation process should lie below the excitation wavelength of the pyridinethiones so that no daylight sensitivity occurs. Because for many experiments on DNA oxidation and strand-breaking processes precursors that absorb at a wavelength of about 350 nm are advantageous, the bond breaking process should be initiated by light with a wavelength of about 350 nm.[27,28]

To find new promising lead structures in the present paper, the parent substance of the thiazolethione precursors is modified systematically. Substituents are not introduced to leave space for further fine-tuning. The heterocycle is modified by substitution of the thiazole sulfur atom by other units. An enumeration of the various systems is summarized in Figure 1. A substitution of the thiazole sulfur atom by a C_2H_2 group leads to the already-known pyridinethiones (**1**). The pyrrole (**3**) heterocycle results from substitution of the sulfur with a CH_2 group whereas the imidazole system (**4**) is obtained if a NH moiety is introduced. An oxygen atom instead of sulfur leads to the oxazole heterocycle (**5**). A substitution of the sulfur by a PH unit generates the phosphazole heterocycle (**6**). Further modifications are obtained by a substitution of the thiocarbonyl group by a carbonyl group. This leads to the hydroxamic acid derivates of the various heterocycles. Whereas the thiohydroxamic acid derivates are indexed by an (**a**), the hydroxamic acid derivates will be indicated by a (**b**). The most prominent examples out of the latter compounds may be the *N*-alkoxypyridine-2(*1H*)-ones (derivatives of *N*-methoxypyridine-2(*1H*)one (**1b**)). They were already successfully employed as photochemical alkoxyl radical sources.[29,30] From the isopropylic ester derivative, for example, isopropyl radicals are generated by an irradiation with light with a wavelength of 300 nm.[28] This is outside the desired range (~350 nm), but nevertheless, the *N*-alkoxypyridine-2(*1H*)-ones allow a further test of our theoretical approach. An in-depth investigation of the photochemistry of the *N*-hydroxypyridine-2(*1H*)one showed that it represents a much cleaner hydroxyl radical source than the *N*-hydroxypyridine-2(*1H*)-thione.[31] Finally, the exchange of the hydroxamic acid N atom with phosphorus results in "phosphothiohydroxamic" acid derivatives, which will be denoted by **c**.

To identify the promising precursor systems, a screening of the lower electronic excitations of all resulting 18 systems (see Figure 1) was performed with TD-DFT employing the B3LYP approach. To check the reliability of the TD-B3LYP, the excitation energies between the ground state (S_0) and the first three singlet excited states were also recalculated with the CASPT2 method. For promising systems, the influence of a polar solvent was estimated by a continuum model. If the CASPT2 confirmed the TD-DFT prediction, the N,O or P,O dissociation paths, respectively, of the S_0, the T_1, and the first two singlet excited states were computed. An analysis of these paths gives information about the reactivity of the resulting radical fragments. Further information is obtained by isodesmic reactions.

Theoretical Details

All DFT and TD-DFT calculations were performed with the TURBOMOLE program package.[32] For the complete active space self-consistent field (CASSCF)[33,34] and CASPT2[19,20] calculations, the MOLCAS program[35] was used.

All vertical excitation energies were computed for theoretically determined ground-state geometries. Because many compounds needed to be screened for this step, the geometries were obtained with the BLYP/SVP[25,26,36] approach. For these calculations, the resolution of identity (RI) approximation[37,38] together with the corresponding auxiliary basis sets[38,39] provided by TURBOMOLE were applied. This approach seems to be sufficient for the screening because, for **1a** and **2a**, the influence of the geometry on the vertical excitation energies was found to be small in comparison to uncertainties arising from the TD-DFT approaches.[18] For the screening, the vertical excitation energies of the five lowest-lying states were obtained with TD-DFT employing the B3LYP functional. In these computations, the TZVP basis sets[40] were applied. To check the solvent effects on the excitation energies, the COSMO[41] approach with a dielectric constant $\epsilon = 78$ was applied. The characters of the strongest absorptions were identified through the shapes of the contributing orbitals. For the most promising systems, the ground-state geometries were reoptimized (RI-MP2/cc-pVTZ[42−44]) and the excitation energies were recalculated employing the CASPT2[19,20] approach. For these calculations, the cc-pVTZ basis sets were used. For all hydrogen atoms and the methoxy carbon atom in *N*-(methoxy)pyridine-2(*1H*)-thione **1a**, the cc-pVDZ basis sets[43,44] had to be employed due to software and hardware limitations. The CASSCF contained the 6 highest occupied and the 6 lowest virtual orbitals (12/12 CAS). For the PT2 computations, the G3 approach[45] for the fock matrix and the multi-state variant of the CASPT2 approach (MS−CASPT2)[46] were used. For the UV/vis absorption spectra, the TD-DFT oscillator strengths were employed. As shown previously for **1a** and **2a**, this approximation is sufficiently accurate for trends.[18]

The calculations for the reaction paths (Figures 2−6) were performed on the CASPT2 level of theory applying the cc-pVTZ

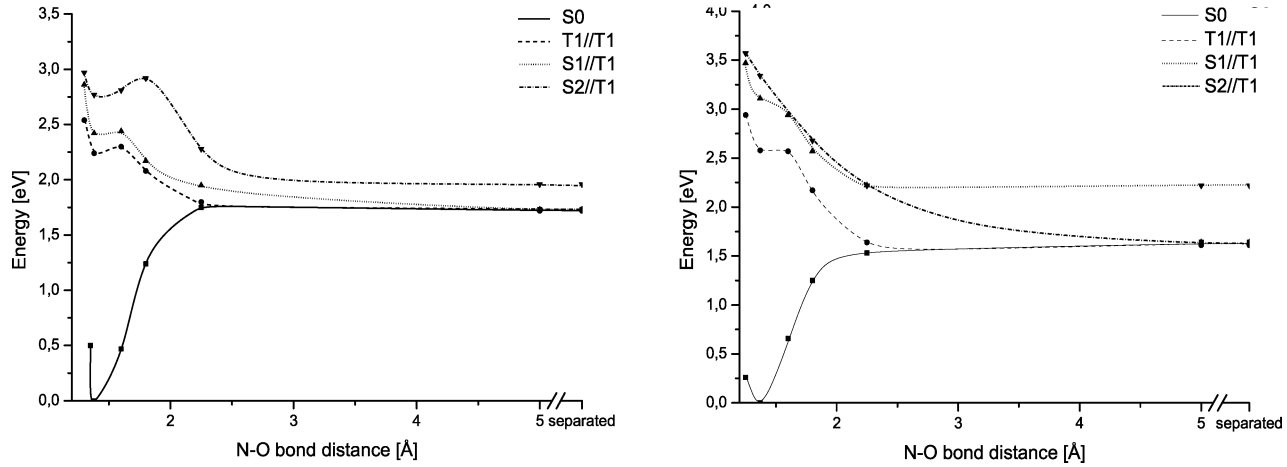

Figure 2. The dissociation pathes of *N*-methoxypyridine-2(*1H*)thione (**1a**) (left) and of *N*-methoxythiazole-2(*3H*)thione (**2a**) (right).

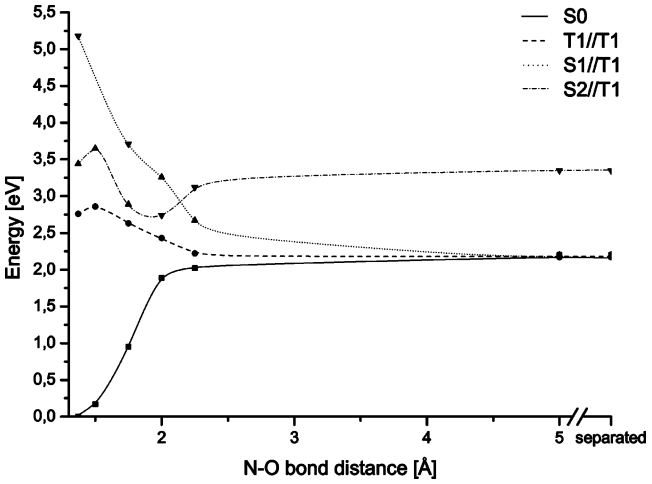

Figure 3. The N,O dissociation pathes of *N*-methoxypyridine-2(*1H*)-one (**1b**).

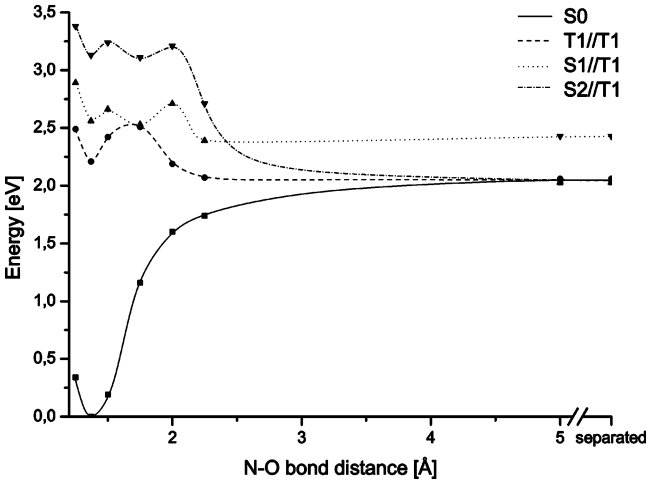

Figure 5. The N,O dissociation pathes of *N*-methoxy-(1,3)dihydro-[1,3]azaphosphole-2-thione (**6a**).

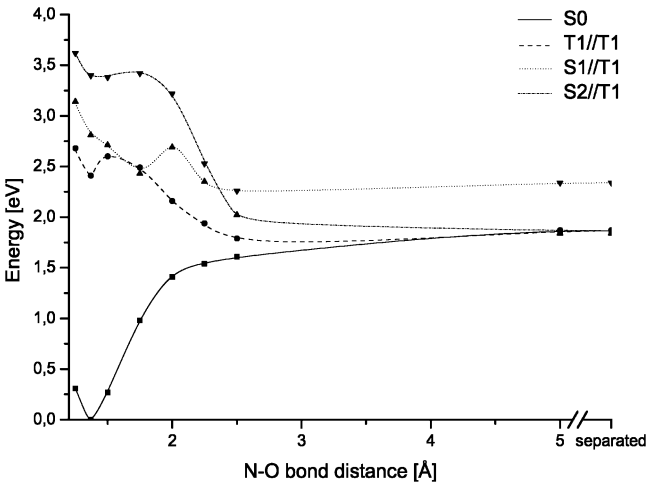

Figure 4. The N,O dissociation pathes of *N*-methoxy-(1,3)dihydro-pyrrole-2-thione (**3a**).

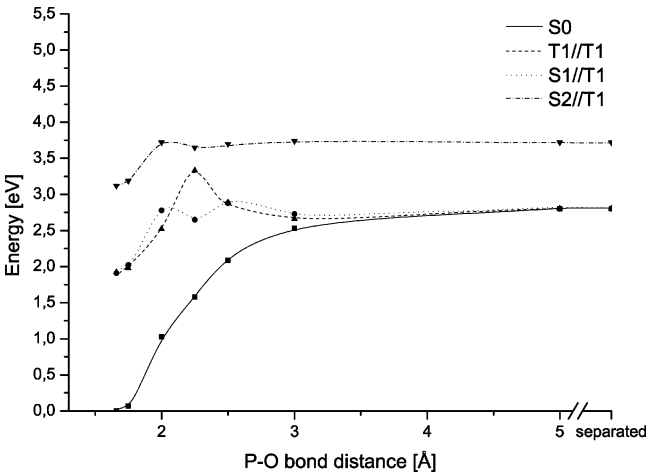

Figure 6. The P,O dissociation pathes of *P*-methoxy-(1,3)dihydro-[1,3]oxaphosphole-2-thione

basis sets. According to our previous calculations, the bond dissociation paths in the S_1 and S_2 states are reasonably described if triplet geometries (T_1 geometry) were employed, at least as long as both fragments interact with each other.[18] Due to this finding for the description of the N,O cleavage (or P,O cleavage in case of the molecules **c**), all internal degrees of freedom of the molecules were optimized at defined N,O (or P,O) bond distances for the S_0 ground-state and the lowest lying triplet state (T_1). These geometry optimizations were performed on the B3LYP/SVP level of theory. For the S_0 geometries, a biradical wave function ($\langle S^2 \rangle = 1$) had to be used at large bond distances to describe the correct fragmentation channel. In our computations, this was achieved with a triplet density matrix as the initial guess. In the following, computations, which involve an optimized geometry for a triplet state, will be abbreviated as $T_1//T_1$, $S_1//T_1$, etc. (i.e. state//optimized geometry). Computations, which use the ground-state geometries, are given as $S_0//S_0$, $T_1//S_0$, etc. For CASSCF and CASPT2

TABLE 1: TD-B3LYP Spectroscopic Data of the $\pi \rightarrow \pi^*$ Excitations of the 18 Molecules Calculated within the Scope of the Screening

	thione (**a**)			ketone (**b**)			phosphoethione (**c**)		
heterocycle	eV	nm	f[a]	eV	nm	f[a]	eV	nm	f[a]
pyridine (**1**)	3.33	373	0.0512	4.21	294	0.0992	2.81	441	0.0818
thiazole (**2**)	4.16	298	0.1336	5.18	239	0.0673	3.08	403	0.0558
pyrrole (**3**)	4.07	305	0.1834	4.82	257	0.0723	3.20	387	0.0215
imidazole (**4**)	4.90	253	0.1998	5.23	237	0.0327	3.47	358	0.1177
oxazole (**5**)	4.77	260	0.1813	5.76	215	0.1117	3.57	347	0.0816
phosphazole (**6**)	3.77	329	0.1387	4.43	280	0.0535	3.18	390	0.0243

[a] Oscillator strength [arbitrary units].

computations of the cleavage processes, an (16/12) active space is necessary because a strong mixing between these orbitals occurs during the bond breaking processes. Consequently, smaller CAS spaces (e.g., in a 12/12 CASSCF) do not allow a reliable description of the photolytical cleavage processes. For the description of the noninteracting methoxyl radical, the results of Höper et al., who applied large scale MR−CI calculations,[47] were used. As an estimate for the maximal excess energies of the resulting radical fragments the differences between the initial vertical $\pi \rightarrow \pi^*$ excitation energies (starting point of the fragmentation process) and the dissociation energy of the S_0 state[48] were taken. The latter determines the energy position of the released radicals in their electronic ground states with respect to the S_0 ground state of the corresponding radical precursors.

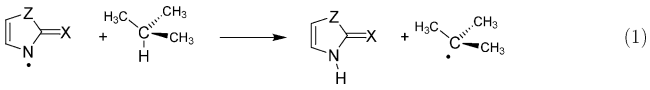

(1)

Equation 1 shows the isodesmic hydrogen abstraction reaction that was applied to estimate the different intrinsic reactivities of the heterocyclic radical fragments and the methoxyl radical. This was done by computing the reaction energies ΔE ($E_{\text{products}} - E_{\text{educts}}$) of this reaction with the radical fragments obtained from the most promissing precurser systems on the B3LYP/TZVP//RI−BLYP/SVP level of theory.

Results and Discussion

Screening Step and More Reliable Computations of the Vertical Excitation Energies. The investigation comprises 18 molecules that were obtained from a systematic modification of *N*-methoxythiazole-2(*3H*)thione (**2a**). They are summarized in Figure 1.

The calculated excitation energies and oscillator strengths of the strong absorptions of all 18 test molecules (TD-DFT; B3LYP/TZVP) are summarized in Table 1. The $\pi \rightarrow \pi^*$ character of these transitions was identified by the shape of the contributing orbitals. All other electronic transitions are less important because they possess vanishing oscillator strengths or do not appear in the window of interest (300−400 nm). They are summarized in the Supporting Information.

This screening reveals the influence of different heteroatoms and functional groups on the UV/vis spectra of these compounds. Taking *N*-methoxythiazole-2(*3H*)thione (**2a**) as a reference system, the influence of the composition of the heterocycle on the energy position of the $\pi \rightarrow \pi^*$ excitation can be seen if the elements of a column of Table 1 are compared. Substituting the sulfur of **2a** by a C_2H_2 group (Z = C_2H_2 instead of Z = S in Figure 1), the already-known and applied *N*-methoxypyridine-2(*1H*)thione (**1a**) is obtained. Both compounds were compared previously.[18] If the sulfur atom of the heterocycle **2a** is replaced by a CH_2 group (Z = CH_2) the pyrrolethione heterocycle **3a** is generated. Its visible $\pi \rightarrow \pi^*$ transition is hardly shifted in comparison to **2a** because the corresponding π and π^* orbitals have the same energy as those of the thiazole compound. Nevertheless, the oscillator strength of this excitation increases in comparison to the reference compound. If the sulfur center is substituted by a NH group (imidazolethione **4a**) or an oxygen center (oxazolethione **5a**), the orbital energies of the virtual π^* orbitals increases. This leads to a blue-shift of the $\pi \rightarrow \pi^*$ excitation by about 50−60 nm (ca. 0.6−0.75 eV). In contrast, the phosphorus (PH) derivative **6a** absorbs at about 329 nm, i.e., possesses a red-shift of about 30 nm (0.4 eV) in comparison to the reference system **2a**.

In addition to the modification of Z, X and Y (see Figure 1) were also varied to screen for promising alkoxyl radical precursors. A replacement of the thiocarbonyl unit by a carbonyl unit (compounds **b**; column 2 in Table 1) leads to hydroxamic acid derivates. As is well-known for other carbonyl and thiocarbonyl systems, the π-orbitals of the carbonyl groups are lower in energy (about 0.2−0.5 eV) than the π-orbitals of the corresponding thiocarbonyl groups.[49] The unoccupied π^*-orbitals raise in energy. This leads to a strong blue-shift of the $\pi \rightarrow \pi^*$ excitation together with a decrease in oscillator strength.

Finally, Y = N was replaced by Y = P (compounds **c**; column 3 in Table 1). This substitution leads to considerable structural changes because the phosphorus center is sp^3 hybridized whereas the nitrogen center is sp^2 hybridized. A a consequence, the P,O bond is bent out of the plane of the heterocycle by about 120°. Due to the substitution, the π- and the π^*-orbitals are both lowered in energy. Because the shifts are larger for the virtual orbitals than for the occupied ones, the $\pi \rightarrow \pi^*$ excitations of the phosphorus derivatives are red-shifted by about 60−100 nm (−0.52 eV for **1** to −1.43 eV for **4**).

These various modifications lead to strong red- (−83 nm; 1.60 eV) and blue- (143 nm; −1.35 eV) shifts with respect to **2a**. One extreme is the oxazole heterocycle in combination with a keto group (**5b**). Its $\pi \rightarrow \pi^*$ excitation lies at 215 nm (5.76 eV). The other extreme is the *P*-methoxy-phosphinine-2(*1H*)-thione (**1c**), which possesses a $\pi \rightarrow \pi^*$ excitation at 441 nm (2.81 eV). This strong bathochromic effect results from the larger π-system of pyridine in combination with the influence of the phosphothiohydroxamic acid group.

According to our last goal (strong absorption at about 350 nm), only 5 of the 18 molecules were selected for a more accurate treatment (**1b, 3a, 4c, 5c, 6a**). Alkoxyl radical precursors are mostly applied in polar solvents. To estimate the influence of a polar solvent on the excitation energies of the visible $\pi \rightarrow \pi^*$ excitation, the COSMO approach ($\epsilon = 78$) was applied in the framework of TD-DFT (Table 2). These calculations showed shifts of only 5−10 nm, which lies within the error bars of the theoretical approach. For thiazolethione precursor systems, the predicted small influence is in line with experimental data.[16,17] In contrast, for pyridinethione **1a**, the computations show a strong blue-shift (−31 nm), but experi-

TABLE 2: Comparison of the TD-B3LYP Spectroscopic Data of the Most Promising Moleclules in Gas Phase and in Solvents[a]

	$n \rightarrow \pi^*$			$\pi \rightarrow \pi^*$		
molecule	gas phase	$\epsilon = 78$[b]	Δ	gas phase	$\epsilon = 78$[b]	Δ
1a	448	388	−60	372	342	−31
2a	356	334	−32	298	291	−7
3a	401	363	−38	305	299	−6
6a	440	402	−38	329	319	−10
1b[c]				294	283	−11
4c	496	458	−38	358	365	7
5c	501	466	−35	347	355	8

[a] All values are in nm. [b] The COSMO model implemented in the TURBOMOLE was used. [c] Because the first electronic excitation is already the $\pi \rightarrow \pi^*$ transition, no values for the $n \rightarrow \pi^*$ transition are given.

TABLE 3: Summary of the 12/12 CASPT2/cc-pVTZ// RI-MP2/cc-pVTZ $\pi \rightarrow \pi^*$ Excitation Energies of the Most Promising Molecules

molecule	eV	nm	experimental value[a]
pyridinethione (**1a**)[b]	3.25	381	359[c] [17]
thiazolethione (**2a**)[b]	3.99	310	320[17]
pyrrolethione (**3a**)	3.79	327	−
phosphazolethione (**6a**)	3.57	348	−
pyridineone (**1b**)	4.00	310	296[53]
azaphospholethione (**4c**)	3.00	414	−
oxaphospholethione (**5c**)	3.52	352	−

[a] Experimental absorption maxima of already measured molecules are also shown. [b] The values for **1a** and **2a** are given for comparison. [c] Maximum of the band.

mental data to support these predictions seems not to be available. For the $n \rightarrow \pi^*$ transition, the influence of a polar solvent is predicted to be much larger (Table 2). However, these transition are less important due to their vanishing oscillator strengths.

To get more accurate information about the $\pi \rightarrow \pi^*$ excitation energy, the first three excited states of the selected molecules were recalculated employing the 12/12 CASPT2/cc-pVTZ//RI-MP2/cc-pVTZ level of theory. The values for the photochemically important $\pi \rightarrow \pi^*$ transitions are summarized in Table 3. The data for all calculated transitions are given in the Supporting Information.

The vertical excitation energies predicted by the CASPT2 approach agree nicely with the maxima of the measured absorption band (deviation 10−20 nm, see Table 3). A comparison of the $\pi \rightarrow \pi^*$ excitation energies from Table 3 (CASPT2) with their corresponding values in Table 3 (TD-DFT/B3LYP) illustrates the uncertainties of TD-DFT methods. For most systems, the TD-DFT values agree nicely (**1a**, **5c**; $\Delta E <$ 0.1 eV) or acceptably (**1b, 2a, 3a, 6a**; $\Delta E <$ 0.25 eV) with the more reliable CASPT2 methods, but for the *P*-methoxy-(1,3)-dihydro-[1,3]azaphosphole-2-thione (**4c**), TD-B3LYP overestimates the $\pi \rightarrow \pi^*$ excitation energy by nearly 0.5 eV (−56 nm). For **4c**, CASPT2 predicts an excitation wavelength of 414 nm (3.00 eV), which lies already well below the desired range. This compound could be of interest for biological studies with living cells because it absorbs in the visible region. However as will been shown for **5c**, a photolytic N,O fragmentation cannot be expected. Therefore its photolytic fragmentation process was not studied.

Evaluation of the Thermal and Photolytic N,O Bond Dissociation Paths to Gain Insight into the Chemical Behavior of the Resulting Fragments. The reactivity of the radicals set free by the photolytic dissociation is determinded from their inherent reactivity and the excess energy which remains deposited in both fragments resulting from the photolytic dissociation process. The maximal excess energy is given as the difference between the $\pi \rightarrow \pi^*$ excitation energy and the dissociation energy of the ground state. The former gives the energy that is deposited in the molecule to initiate the homolytic N,O fragmentation, whereas the latter determines the energy position of the fragments with respect to the starting point of the process. The real remaining excess energy is much smaller than the maximal excess energy because energy dissipates to the solvent.[21] Assuming that the rates of the dissipation are very similar for the molecules under consideration, differences in the real excess energy of the radical fragments only depend on the maximal excess energies and the time needed for the fragmentation process. In our previous work,[18] this simple model was indeed able to explain the differences in the reactivity of the alkoxyl radicals obtained from a photolytic fragmentation of *N*-methoxypyridine-2(*1H*)thione (**1a**) and *N*-methoxythiazole-2(*3H*)thione (**2a**).

The maximal excess energies and estimates about the time scales for the respective photolytic N,O homolyses of **1a** and **2a** were obtained from the shapes of the computed $S_0//S_0$, $S_1//T_1$, $S_2//T_1$, and $T_1//T_1$ potential curves given in Figure 2. The maximal excess energy of **1a** (Figure 2 left-hand side, Table 4) is 147 kJ mol^{-1}, whereas 226 kJ mol^{-1} was computed for **2a** (Figure 2 right-hand side, Table 4). The shapes of the potential curves also show that, for **2a**, the photolytic fragmentation can occur via a perfect slide reaching from the starting point (vertical $\pi \rightarrow \pi^*$ excitation) to the end point. Therefore, the time needed for the process can be expected to be small. For **1a**, much more time is needed because no direct connection exists. The higher maximal excess energy and the faster photolytic fragmentation process, leading to a smaller amount of energy dissipation to the solvent, nicely explains the much higher reactivity of the fragments of **2a** in comparison to those of **1a**.

In addition to this estimate, in the present study, we also investigate the intrinsic chemical reactivity of the resulting radical fragments. Such information is obtained by computing the reaction energies ΔE ($E_{\text{products}} - E_{\text{educts}}$) of the isodesmic hydrogen abstaction reaction shown in eq 1. The investigated C,H bond in isobutane has a bonding energy of 380 kJ mol^{-1}.[50] The two positive reaction energies of 44 kJ mol^{-1} (**1a**) and 56 kJ mol^{-1} (**2a**) indicate that the heterocyclic radical fragments resulting from the photochemical dissociation process of **1a** or **2a** are not able to abstract the indicated hydrogen of isobutane and that **1a** leads to the slightly more reactive heterocyclic radical fragment than **2a**. This shows that the inherent reactivity of the fragments does not explain the experimentally found differences. Additionally, by comparing the small difference in the reaction energies of the isodesmic reactions with the large difference in the estimated maximal excess energies, it is clear that the latter will still be mainly responsible for the differences in the chemical behavior of the fragments. This holds even if the difference is largely dimished by quenching processes. The reaction energy for the isodesmic reaction (eq 1) of isobutane with the resulting methoxyl radical ($CH_3O\cdot$) is about −28 kJ mol^{-1}, underlining its stronger reactivity in comparison to the heterocyclic radical fragments.

The experimental data known for the *N*-alkoxypyridine-2(*1H*)ones[28−30] opens the possibility to test if our model also holds for a wider range of molecules. The potential curves of *N*-methoxypyridine-2(*1H*)one (**1b**) are summarized in Figure 3. In contrast to **1a** and **2a**, for **1b**, the S_1 state is expected to be populated by an irradiation of the molecule with UV/vis light.

TABLE 4: Summary of the Data for the Description of the Photolytical Radical Liberation Process and the Chemical Behavior of the Radical Fragments[a]

	excitation energy[a]		dissociation energy[b]		maximal excess energy[c]		barrier for the dissociation[d]		isodesmic reaction[e]
molecule	eV	nm	eV	kJ mol^{-1}	eV	kJ mol^{-1}	eV	kJ mol^{-1}	ΔE kJ mol^{-1}
pyridinethione (**1a**)	3.25	381	1.73	166.8	1.52	146.6	0.11	10.6	44.4
thiazolethione (**2a**)	3.99	310	1.65	159.1	2.34	225.7			56.1
pyrrolthione (**3a**)	3.79	327	1.84	177.4	1.95	188.1	< 0.05	< 5.0	24.1
phosphazolethione (**6a**)	3.57	348	1.89	182.3	1.68	162.0	0.10	9.6	22.3
pyridineone (**1b**)	4.00	310	2.20	212.2	1.80	173.6	0.21	20.2	−6.6
oxaphospholethione (**5c**)	3.52	352	2.80	270.0	0.72	69.4	no dissociation		

[a] The vertical $\pi \rightarrow \pi^*$ excitation energies calculated on the 12/12 CASPT2/cc-pVTZ//RI-MP2/cc-pVTZ level of theory. [b] The S_0 dissociation energies computed on the 16/12 CASPT2/cc-pVTZ//RI-MP2/cc-pVTZ level of theory.[48] [c] The difference between the initial vertical $\pi \rightarrow \pi^*$ excitation energy (starting point of the fragmentation process) and the dissociation energy of the S_0 state.[48] [d] The highest barrier toward the N,O bond homolysis in the photochemical active state (the S_1 state in the case of (1b), the S_2 state for the other systems). [e] ΔE ($E_{products} - E_{educts}$) values for the isodesmic hydrogen abstraction reaction shown in eq 1. The value for the methoxylradical is $\Delta E = -27.9$ kJ mol^{-1}.

From the dissociation energy of the ground state and the vertical $S_0 \rightarrow S_1$ transition, a maximal excess energy of 174 kJ mol^{-1} is obtained, which falls between the values obtained for **1a** and **2a**. On the way to the N,O fragmentation along the S_1 curve, molecule **1b** will be trapped in a quite-deep minimum (the depth with respect to the dissociation is about 0.4 eV) from which it can cross (via spin−orbit coupling) to the triplet surface. Despite the small spin−orbit coupling expected for first row elements, the transfer should be efficient because both states come close in energy. From the T_1 state, it easily fragments into the desired radicals because the T_1 state is repulsive in that region. Nevertheless, due to the time needed for the singlet triplet transfer, a large amount of excess energy should dissipate to the solvent. Summarizing, the curves shown in Figure 3 predict that **1b** is a clean photochemical source of alkoxyl radicals, which is indeed found experimentally.[28−30] The isodesmic reaction indicates that the resulting pyridyl-2-onyl radicals ($\Delta E = -6.6$ kJ mol^{-1}) are considerably more reactive than the pyridyl-2-thionyl radical ($\Delta E = 44.4$ kJ mol^{-1}), which results from the fragmentation of **1a**. However, as we already pointed out, this should be less important than the remaining excess energy.

To obtain similar information for the new promissing systems (**3a**, **6a**, **5c**) the N,O dissociation paths (P,O in the case of **5c**) were analyzed to compute the maximal excess energies of the radical fragments and to obtain information about a possible dissipation of this excess energy. The obtained data are summarized in Table 4, which also contains the highest of possible barriers in the S_2 state and the reaction energies of the calculated isodesmic reactions with isobutane. The corresponding potential curves are given in Figures 4−6. In these figures, the lines connect those eigenvalues of the hamilton matrix that possess similar electronic characters (approximated diabatic representation). The symbols themselves indicate the energy order of the eigenvalues (adiabatic approximation). This was made to pronounce possible avoided crossings. The CASPT2 method was employed throughout.

The N,O dissociation paths of *N*-methoxy-(1,3)dihydro-pyrrole-2-thione (**3a**) for the $S_0//S_0$, $T_1//T_1$, $S_1//T_1$, and the $S_2//T_1$ states are shown in Figure 4. **3a** has a thermal N,O dissociation energy of 178 kJ mol^{-1}. The photochemical process is most probably initiated by an excitation into the S_2 state because only the $S_0 \rightarrow S_2$ transition exhibits a significant oscillator strength (Table 1, Supporting Information). From the difference of the dissociation energy (178 kJ mol^{-1}; 1,84 eV) and the vertical excitation energy (3.79 eV), a maximal excess energy of 188 kJ mol^{-1} is computed for the released radicals in their electronic ground states. This is slightly higher than the corresponding value of **1a** but considerably lower than for **2a**.

The S_2 state possesses only a very small barrier (<5 kJ mol^{-1}) toward the N,O fragmentation so it can be expected that the N,O bond dissociation takes place after the excitation process. Similar to **2a**, the fragmentation will lead to the radical fragments in their ground states (pyrryl-2-sulfanyl radical, methoxyl radical in its degenerated ^{2}E state) because at a N,O distance of 2.5 Å, the S_2 state crosses with the S_1 state. Due to the fast process, only a smaller amount of excess energy should dissipate to the solvent, i.e., the reactivity of the resulting fragments is expected to lie between **1a** and **2a**. Only if a direct fragmentation from the S_2 will not occur much of the maximal excess energy can dissipate because a de-excitation to the S_1 followed by the fragmentation from the S_1 involves a barrier or a further decay to the T_1 state. Both processes occur on a longer time scale and allow a dissipation of excess energy. The reaction energy ΔE for the isodesmic reaction of the pyrryl-2-sulfanyl radical with isobutane is 24.1 kJ mol^{-1}, i.e., it possesses a higher intrisic chemical reactivity than the heterocyclic radical fragments of **1a** and **2a**.

The thermal and photochemical paths for the homolytic N,O bond cleavage of *N*-methoxy-(1,3)dihydro-[1,3]azaphosphole-2-thione (**6a**) are depicted in Figure 5. The maximal excess energy of the fragments is 162 kJ mol^{-1}, which is only slightly higher than the value computed for **1a** (147 kJ mol^{-1}). A direct fragmentation out of the S_2 is hindered by barriers and also the S_1 curve is not repulsive. Therefore, it can be expected that the excess energy will be dissipated to some extend regardless if the fragmentation occurs directly from the S_2 or from the S_1 state. The isodesmic reaction (eq 1) of the heterocyclic [1,3]-azaphosphyl-2-sulfanyl radical fragment gives a ΔE value of 22.3 kJ mol^{-1}, showing that it is more reactive than the fragment of **1a**. However, taking into account that the maximal excess energy of the photolytic fragmentation and its dissipation is the dominant effect, the radical fragments resulting from a N,O cleavage of **6a** are expected to be only slightly more reactive than those obtained from **1a** due to the higher maximal excess energy and a higher intrinsic reactivity.

(2)

The phosphazole (**6**) heterocycle possess tautomeric forms (eq 2), which have to be taken in account.

TABLE 5: Energy Differences (kJ mol^{-1}) between Both Tautomeric Forms of 6a (eq 2) Calculated with Different Methodes

method	Δ(**taut-6a** − **6a**)
B3LYP/TZVP//RI−BLYP/SVP	−10.9
RI-MP2/cc-pVTZ	−24.4
RICC2/cc-pVTZ//RIMP2/cc-pVTZ	−19.5
B3LYP/TZVP/ϵ=30//RI−BLYP/SVP/ϵ=30	−7.1
B3LYP/TZVP/ϵ=78//RI−BLYP/SVP/ϵ=78	−6.9

TABLE 6: TD-B3LYP Data for the Electronic Spectra of the Tautomeric Form of 6a (taut-6a)

eV	nm	f^a	contributing orbitals^b	
4.36	284	1.54×10^{-2}	38 → 40	68.2
			38 → 39	29.4
4.80	259	1.30×10^{-1}	38 → 39	56.8
			38 → 40	29.3
4.92	252	1.77×10^{-2}	38 → 41	46.6
			38 → 42	44.4
5.19	239	1.78×10^{-2}	37 → 39	35.3
			38 → 42	31.1
			38 → 41	29.0
5.63	220	1.69×10^{-2}	37 → 40	76.0
			37 → 39	12.5

[a] Oscillator strength [arb. units]. [b] The orbital transitions contributing to the calculated electronic excitation. Contributions with a weight below 10% are not shown. A characterization of the orbitals in terms of n, π, and π* was not done because the orbitals possess a completely different character here than in compound **6a**.

The energy difference between the two tautomeric forms was calculated on different levels of theory. All approaches predict the thiol form of **6a** (**taut-6a**) to be lower in energy than the thione form (Table 5). A polar environment seems to lessen the energy differences, but even in water ($\epsilon = 78$), only traces of the thione form will exist. Excitation energies, oscillator strengths, and characterizations of the five lowest lying vertical excitations of the thiole form **taut-6a** are summarized in Table 6. As expected, the spectrum does not resemble the one of the thione form. The lowest excitation lies at about 280 nm, i.e., much higher than the desired range.

Therefore, the phosphor has to be methylated (**meth-6a**) to yield the desired properties. To investigate to what extent a methylation of the phosphor center of **6a** influences the energy position of the electronically excited states, we computed the five lowest excitation energies of *N*-methoxy-3-methylazaphosphole-2-thione (**meth-6a**) (Table 7). As expected, the spectra of **6a** and **meth-6a** are very similar. The $\pi \rightarrow \pi^*$ excitation, which remains the most intensive band, is red-shifted by only 5 nm. With the utmost probability, the N,O fragmentation paths of **6a** and **meth-6a** will also be very similar. Therefore, the calculation of the ones of **meth-6a** was omitted.

In the case of the *P*-methoxy-(1,3)dihydro-[1,3]oxaphosphole-2-thione **5c**, the bond breaking process involves the P,O bond. As expected, the potential curves of the homolytic P,O cleavage in the various states (Figure 6) possess completely different shapes than those obtained for the other compounds. Figure 6 clearly indicates that neither a population of the S_1 nor of the S_2 state will lead to a cleavage of the P,O bond. Consequently, a fragmentation to an alkoxyl and an oxaphosphyle radical cannot be expected. We assume that the potential curves of **4c** that possessed a very low $S_0 \rightarrow S_2$ excitation energy are very similar to those of **5c**. Therefore, also, **4c** cannot be expected to be an efficient alkoxyl radical precursor.

Conclusion

The present work performs a computer-aided design of new alkoxyl radical precursors. Combining the advantages of *N*-alkoxypyridine-2(*1H*)thiones and *N*-alkoxythiazole-2(*3H*)-thiones the radical formation should be initiated by an irradiation with light at about 350 nm, and the amount of side products during the radical formation process should be small even in the absence of radical trapping reagents. To predict the properties of new test candidates, a protocol was employed which was already successful in rationalizing the differences between the properties of *N*-methoxypyridine-2(*1H*)thione (**1a**) and *N*-methoxythiazole-2(*3H*)thione (**2a**).[18] The protocol was tested on *N*-methoxypyridine-2(*1H*)one **1b**, who's properties are already known experimentally. This test supports that our model indeed captures the most important effects.

Eighteen test candidates were obtained by a systematic variation of the parent compound of the thiazolethione precursor. Possible effects of substituents were not taken into account to leave space for further fine-tuning. The influence of a polar solvent was also tested but turned out to be less important for the vissible $\pi \rightarrow \pi^*$ excitation of the interesting molecules. From the 18 test molecules, the methylated form **meth-6a** of *N*-methoxy-(1,3)dihydro-[1,3]azaphosphole-2-thione (**6a**) and *N*-methoxy-(1,3)dihydro-pyrrole-2-thione (**3a**) seem to be the most promising candidates. For **meth-6a**, the computations predict a strong absorption at about 350 nm, leading to alkoxyl radicals that should yield only a small amount of side products during their formation process. The $S_0 \rightarrow S_2$ transition of *N*-methoxy-(1,3)dihydro-pyrrole-2-thione (**3a**) lies at about 330 nm, and the released radicals should be only slightly more reactive than those obtained from **1b**, which is known as a clean photochemical source of alkoxyl radicals.

Acknowledgment. We thank I. Fischer and J. Hartung for the valuable discussions.

Supporting Information Available: Cartesian coordinates of all RI−BLYP/SVP optimized molecules within in the scope of the screening. Characterization of the TD-DFT B3LYP/TZVP excited states within the scope of the screening. RIMP2/cc-pVTZ geometries (Cartesian coordinates), CASSCF and CASPT2 energies of the ground state and the first three singlet excited

TABLE 7: TD-B3LYP Data for the Electronic Spectra of the Methylated Molecule (meth-6a) and 6a

meth-6a					**6a**				
eV	nm	f^a	contibuting orbitals^b		eV	nm	f^a	contibuting orbitals^b	
2.82	439	4.59×10^{-4}	n → π*	80.7	2.82	440	4.93×10^{-4}	n → π*	90.1
3.71	334	1.40×10^{-1}	$\pi \rightarrow \pi^*$	78.4	3.77	329	1.39×10^{-1}	$\pi^* \rightarrow \pi^*$	86.8
4.81	258	2.51×10^{-3}	n → $LUMO_{+1}$	84.9	4.79	259	1.10×10^{-2}	n → $LUMO_{+1}$	93.8
4.99	248	2.88×10^{-2}	$\pi \rightarrow LUMO_{+1}$	70.3	4.85	255	4.78×10^{-4}	$\pi \rightarrow LUMO_{+1}$	86.0
4.72	263	2.64×10^{-2}	HOMO-2 → π*	72.0	5.01	247	1.26×10^{-2}	n → LUMO+2	79.5

[a] Oscillator strength [arb. units]. [b] The orbital transitions contributing to the calculated electronic excitation. Contributions with a weight below 10% are not shown.

states of the most promising systems. B3LYP/SVP geometries (Cartesian coordinates), and CASPT2 energies of the $S_0//S_0$, $T_1//T_1$, $S_1//T_1$, and the $S_2//T_1$ states calculated for the description of the dissociation processes. Geometries and energies for **taut-6a** and **meth-6a**. B3LYP/TZVP//RI−BLYP/SVP geometries and energies for the isodesmic reactions. This material is available free of charge via the Internet at http://pubs.acs.org.

References and Notes

(1) Adam, W.; Hartung, J.; Okamoto, H.; Saha-Möller, C. R.; Špehar, K. *Photochem. Photobiol.* **2000**, *72*, 619−624.

(2) Möller, M.; Adam, W.; Marquardt, S.; Saha-Möller, C. R.; Stopper, H. *Free Radical Biol. Med.* **2005**, *39*, 437−482.

(3) Aveline, B. M.; Redmond, R. W. *Photochem. Photobiol.* **1998**, *68*, 266−275.

(4) Adam, W.; Grimm, G. N.; Saha-Möller, C. R. *Free Radical Biol. Med.* **1998**, *24*, 234−238.

(5) Hartung, J.; Gallou, F. *J. Org. Chem.* **1995**, *60*, 6706−6716.

(6) Hartung, J.; Gottwald, T.; Špehar, K. *Synthesis* **2002**, 1469−1498.

(7) Hartung, J.; Hiller, M.; Schmidt, P. *Chem.—Eur. J.* **2001**, *2*, 1014−1023.

(8) Hartung, J. *Eur. J. Org. Chem.* **2001**, 619−632.

(9) Renaud, P.; Gerster, M. *Angew. Chem.* **1998**, *110*, 2704−2722.

(10) Porter, N.; Giese, B.; Curran, D. *Acc. Chem. Res.* **1991**, *24*, 296−304.

(11) Esker, J.; Newcomb, M. *Adv. Heterocycl. Chem.* **1993**, *58*, 1−45.

(12) Boivin, J.; Crépon, E.; Zard, S. Z. *Tetrahedron Lett.* **1990**, *31*, 6869−6872.

(13) Aveline, B. M.; Kochevar, I. E.; Redmond, R. W. *J. Am. Chem. Soc.* **1995**, *117*, 9699−9708.

(14) Hartung, J.; Hiller, M.; Schwarz, M.; Svoboda, I.; Fuess, H. *Liebigs Ann.* **1996**, 2091−2097.

(15) Hartung, J.; Kneuer, R. *Eur. J. Org. Chem.* **2000**, 1677−1683.

(16) Hartung, J.; Schwarz, M.; Svoboda, I.; Fuess, H.; Duarte, M. *Eur. J. Org. Chem.* **1999**, 1275−1290.

(17) Hartung, J.; Špehar, K.; Svoboda, I.; Fuess, H.; Arnone, M.; Engels, B. *Eur. J. Org. Chem.* **2005**, 869−881.

(18) Arnone, M.; Hartung, J.; Engels, B. *J. Phys. Chem. A* **2005**, *109*, 5943−5950.

(19) Andersson, K.; Malmqvist, P.-Å.; Roos, B. O. *J. Chem. Phys.* **1992**, *96*, 1218−1226.

(20) Andersson, K.; Malmqvist, P.-Å.; Roos, B. O.; Sadley, A. J.; Wolinski, K. *J. Phys. Chem.* **1990**, *94*, 5483−5488.

(21) Estimates show that in a direct dissociation along a repulsive coordinate 50−80% of the excess energy remains on the fragments. Most of the excess energy is transformed into translation energy. Because the translation energy is distributed according to the conservation of momentum, the lighter fragment will gain more translation energy.[51,52]

(22) Bauernschmitt, R.; Ahlrichs, R. *J. Am. Chem. Soc.* **1998**, *120*, 5052−5059.

(23) Bauernschmitt, R.; Ahlrichs, R. *Chem. Phys. Lett.* **1996**, *256*, 454−464.

(24) Becke, A. D. *J. Chem. Phys.* **1993**, *98*, 5648−5652.

(25) Lee, C.; Yang, W.; Parr, R. G. *Phys. Rev. B.* **1988**, *37*, 785−789.

(26) Becke, A. D. *Phys. Rev. A.* **1988**, *38*, 3098−3100.

(27) Adam, W.; Grimm, G. N.; Marquardt, S.; Saha-Möller, C. R. *J. Am. Chem. Soc.* **1999**, *121*, 1179−1185.

(28) Adam, W.; Hartung, J.; Okamoto, H.; Marquardt, S.; Nau, W. N.; Pischel, U.; Saha-Möller, C. R.; Špehar, K. *J. Org. Chem.* **2002**, *67*, 6041−6049.

(29) Adam, W.; Marquardt, S.; Kemmer, D.; Saha-Möller, C. R.; Schreier, P. *Photochem. Photobiol. Sci.* **2002**, *1*, 609−612.

(30) Adam, W.; Marquardt, S.; Kemmer, D.; Saha-Möller, C. R.; Schreier, P. *Org. Lett.* **2002**, *4*(2), 225−228.

(31) Aveline, B. M.; Kochevar, I. E.; Redmond, R. W. *J. Am. Chem. Soc.* **1996**, *118*, 10124−10133.

(32) Ahlrichs, R.; Bär, M.; Baron, H.-P.; Bauernschmitt, R.; Böcker, S.; Ehrig, M.; Eichkorn, K.; Elliott, S.; Haase, F.; Häser, M.; Horn, H.; Huber, C.; Huniar, U.; Kattannek, M.; Kölmel, C.; Kollwitz, M.; Ochsenfeld, C.; Öhm, H.; Schäfer, A.; Schneider, U.; Treutler, O.; von Arnim, M.; Weigend, F.; Weis, P.; Weiss, H. TURBOMOLE; Quantum Chem. Group: University of Karlsruhe, Germany, 1988.

(33) Roos, B. O.; Taylor, P. R.; Siegbahn, P. E. M. *Chem. Phys.* **1980**, *48*, 157−173.

(34) Roos, B. O. In *Adv. Chem. Phys.*; Laweley, K., Ed.; John Whyley & Sons Ltd.: Chester, England, 1987; p 139.

(35) MOLCAS version 5. Andersson, K.; Barysz, M.; Bernhardsson, A.; Blomberg, M. R. A.; Cooper, D. L.; Fleig, T.; Fülcher, C. M.; de Graaf, C.; Hess, B. A.; Karlström, G.; Lindh, R.; Malmqvist, P.-Å.; Neogrády, P.; Olsen, J.; Roos, B. O.; Sadley, A. J.; Schütz, M.; Schimmelpfennig, B.; Seijo, L.; Serrano-andrés, L.; Siegbahn, P. E. M.; Stålring, J.; Thorsteinsson, T.; Veryazov, V.; Widmark, P.-O. Lund University: Sweden, 2000.

(36) Schäfer, A.; Horn, H.; Ahlrichs, R. *J. Chem. Phys.* **1992**, *97*, 2571−2577.

(37) Vahtras, O.; Almlöf, J.; Feyereisen, W. *Chem. Phys. Lett.* **1993**, *213*, 514−518.

(38) Eichkorn, K.; Treutler, O.; Öhm, H.; Häser, M.; Ahlrichs, R. *Chem. Phys. Lett.* **1995**, *242*, 652−660.

(39) Eichkorn, K.; Treutler, O.; Öhm, H.; Häser, M.; Ahlrichs, R. *Chem. Phys. Lett.* **1995**, *240*, 283−290.

(40) Schäfer, A.; Huber, C.; Ahlrichs, R. *J. Chem. Phys.* **1992**, *100*, 5829−5835.

(41) Klamt, A.; Schüurmann, G. J. *J. Chem. Soc., Perkin Trans. 2* **1993**, *2*, 799−805.

(42) Weigend, F.; Hätting, C.; Köhn, A. *J. Chem. Phys.* **2002**, *116*, 3175−3183.

(43) Woon, D.; Dunning, T. H. J. *J. Chem. Phys.* **1993**, *98*, 1358−1371.

(44) Dunning, T. H. J. *J. Chem. Phys.* **1989**, *90*, 1007−1023.

(45) Andersson, K. *Theor. Chim. Acta* **1995**, *91*, 31−46.

(46) Finley, J.; Malmqvist, P.-Å.; Roos, B. O.; Serrano-Andres, L. *Chem. Phys. Lett.* **1998**, *288*, 299−306.

(47) Höper, U.; Botschwina, P.; Köppel, H. *J. Chem. Phys.* **2000**, *112*, 4132−4142.

(48) For the computations employing the CASPT2 approach the dissociation energies were computed as the difference between the equilibrium geometries and $R_{bond} = 5$ Å.

(49) Farnworth, E. R.; King, G. W.; Moule, D. C. *Chem. Phys.* **1973**, *1*, 82−88.

(50) Williams, J. M.; Hall, W. H. *J. Chem. Phys.* **1968**, *49*, 4467−4477.

(51) Schinke, R. *Photodissociation Dynamics*; Cambridge University Press: Cambridge, UK, 1993.

(52) Ellen, C. G.; Crim, F. F. *Annu. Rev. Phys. Chem.* **2006**, *57*, 273−302.

(53) Gardner, J. N.; Katritzky, A. R. *J. Chem. Soc.* **1957**, 4375−4385.